A Non-Antibacterial Oxazolidinone Derivative that Inhibits Epithelial Cell Sheet Migration

Kevin T. Mc Henry, Sudha V. Ankala, Arun K. Ghosh, and Gabriel Fenteany*[a]

We have developed a high-throughput assay for screening chemical libraries for compounds that affect cell sheet migration during wound closure in epithelial cell monolayers. By using this assay, we have discovered a new inhibitor of cell sheet migration. This compound (UIC-1005) is a 3,4-disubstituted oxazolidinone that bears an electrophilic α,β-unsaturated N*-acyl group required for activity. UIC-1005 also inhibits growth in an epithelial cell proliferation assay. The molecule does not display general toxicity at concentrations at which it potently inhibits cell sheet migration and growth. Unlike certain 3,5-disubstituted oxazolidinones, it exhibits no antibacterial activity. UIC-1005 therefore represents a new class of bioactive oxazolidinone derivative that may prove useful as a probe for signaling pathways leading to cell motility.*

KEYWORDS:

cell migration · high-throughput screening · inhibitors · oxazolidinone · wound closure

Introduction

Cell shape change and motility are critical components of a range of biological processes in animals, including embryonic development, tissue repair, angiogenesis, and immune system function. Cell migration is also involved in pathological events such as cancer metastasis. While a great deal of progress has been made in the last decade in identifying components of signal transduction pathways leading to cell motility, a complete model of the mechanism is still lacking. The precise roles of many of the proteins implicated in these pathways are not yet clear, and there may be a number of mechanisms that cells can use for movement.

Cell motility is dependent on regulated actin filament assembly, rearrangement, and disassembly. A large and growing number of proteins are known to regulate and modulate the state of the actin cytoskeleton, and some appear to have partly overlapping functions.[1–10] For example, actin polymerization and filament assembly can be accomplished through de novo nucleation of new filaments by the actin-related protein (Arp) 2/3 complex or through elongation of existing filaments at free barbed (or fast-growing) ends, which are generated by filament severing and/or regulated dissociation of bound barbed-end capping proteins (uncapping). Similarly, there are multiple routes to actin filament bundling, cross-linking, and disassembly (depolymerization).

A number of different upstream signaling pathways leading to changes in the state of the actin cytoskeleton and cell morphology and behavior have come to light. In particular, the Ras-related small guanosine triphosphatases (GTPases) of the Rho family, which includes Rac, Rho, and Cdc42, have been implicated in the regulation of the actin cytoskeleton and cell shape, and each plays a distinct and specialized role.[11–14] Rho proteins, such as RhoA, are generally associated with formation of contractile actin/myosin bundles, stress fibers, and focal adhesions. Rac proteins, especially Rac1, are associated with membrane ruffling and the formation of lamellipodia (broad, sheet-like membrane protrusions at the leading edge in the direction of movement). Lamellipodial cell crawling resulting from Rac activation is considered to be the most prevalent form of animal-cell motility. Cdc42 is associated with formation of filopodia (finger-like membrane protrusions) and the control of cell polarity. The Rho-family small GTPases also have roles in many other cellular processes, including cell growth[15–17] and cell–cell adhesion.[18] In addition to these small GTPases, phosphoinositides and calcium are known to regulate actin dynamics and cell migration.[19] However, a comprehensive understanding of the signaling cascades leading to cell motility and the relationship between these regulators remains elusive. Progress in this field would be facilitated by the availability of more pharmacological probes of cell motility.

Few small molecules are presently known that affect actin dynamics and cell motility by inhibiting specific actin-regulatory and actin-binding proteins; however, many compounds have been discovered that target actin directly.[20] The best known are the cytochalasins, cell-permeant destabilizers of actin filaments, and phalloidin, a cell-impermeant stabilizer of actin filaments.[21] Other actin-targeted small molecules include the latrunculins, cell-permeant disrupters of actin filaments,[22] and jasplakinolide, a cell-permeant stabilizer of actin filaments.[23] In addition, a few compounds are known that target components upstream of the actin cytoskeleton,[20] such as the Rho-associated kinase inhibitor Y-27632[24] and myosin light chain kinase inhibitors such as ML-

[a] *Prof. G. Fenteany, K. T. Mc Henry, Dr. S. V. Ankala, Prof. A. K. Ghosh*
Department of Chemistry
University of Illinois at Chicago
Chicago, IL 60607 (USA)
Fax: (+1) 312-996-0431
E-mail: fenteany@uic.edu

  1439-4227/02/03/11 $ 20.00+.50/0

9.[25] Recently, a cyclic peptide dimer was discovered that inhibits the activity of N-WASP, a protein involved in Cdc42-mediated actin nucleation by the Arp2/3 complex.[26] Nevertheless, there is a paucity of cell-permeant small molecules currently available that target actin-regulatory and actin-binding proteins.

We have developed a system for rapidly screening chemical libraries for compounds that inhibit or accelerate epithelial cell sheet migration. The system is a scrape-wound closure assay using cultured Madin – Darby Canine Kidney (MDCK) epithelial cell monolayers. Wound closure in this system is driven mainly by cell spreading and migration and not by cell proliferation.[27–29] This wound closure assay can be performed in parallel on multiwell tissue culture plates and analyzed rapidly. Mechanical scraping of the epithelial cell monolayer induces cell sheet migration into the resulting gap, a phenomenon characteristic of wounded epithelia and mechanistically related to normal epithelial movements during embryonic morphogenesis.[30] Epithelial cell sheet migration in this system proceeds by a Rac- and phosphoinositide-dependent cell crawling mechanism resembling the motility of other animal cells that move as individuals rather than as cell sheets.[28]

By screening a collection of synthetic molecules in parallel with this epithelial wound closure assay system, we discovered a novel inhibitor of cell sheet migration. We also found that this molecule inhibits cell proliferation in a separate assay. This compound (UIC-1005) is biologically active at concentrations at which there is no general toxicity, as determined by Trypan Blue exclusion, morphological observations, formation of new actin bundles at the wound margin, and reversibility of the compound's biological effects. UIC-1005 is a 3,4-disubstituted oxazolidinone with an electrophilic α,β-unsaturated *N*-acyl group ("Michael acceptor") required for activity, a fact suggesting a possible mode of action (Scheme 1). Unlike certain chemically distinct 3,5-disubstituted oxazolidinones such as linezolid, UIC-1005 does not have antibacterial activity against either Gram-positive or Gram-negative bacteria. The present study therefore defines UIC-1005 as a new type of inhibitor of eukaryotic cell migration and growth.

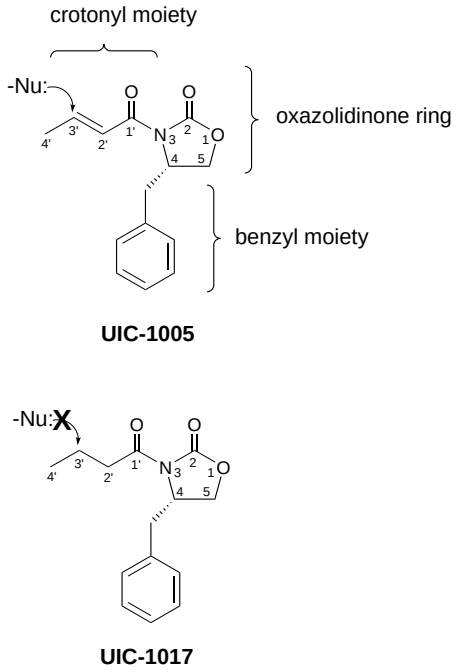

Scheme 1. *Structures of UIC-1005 and UIC-1017. A putative mechanism of action is presented in which a nucleophilic target adds to the electrophilic α,β-unsaturated acyl (crotonyl) group of UIC-1005. This unsaturated moiety is lacking in UIC-1017.*

Results and Discussion

Closure of scrape wounds in MDCK cell monolayers is driven primarily by cell spreading and cell motility and not cell proliferation, based on analysis of cell behavior during wound closure, measurement of proliferation, and experimental treatments that block cell growth without inhibiting closure.[27–29] Similar results were obtained in monkey renal epithelial cells.[31] Wound closure in the MDCK system involves Rac- and phosphoinositide-dependent actin polymerization and protrusive cell crawling, and generation of motile force is distributed along multiple rows of cells from the wound margin in the migrating cell sheet.[28]

Scrape wounds of consistent size can be made easily in MDCK cell monolayers cultured in multiwell tissue culture plates, which makes this assay scalable to high-throughput formats. The progress of wound closure, which is directly driven by protrusive cell motility,[28] can be readily followed. This wound closure assay is therefore an excellent system for rapid screening of chemical libraries for compounds that affect cell sheet migration, as described in the Experimental Section. A similar wound closure assay with human esophageal cancer cells was employed in a qualitative primary screen to identify a new *Streptomyces* natural product, named migrastatin, that inhibits tumor cell migration[32] and cell proliferation.[33] However, these cells tend to break away from the wound edge and migrate into the wounded area not as a continuous sheet but as single cells, whereas MDCK cells maintain cell – cell contacts and a stable wound margin; they move into the denuded area as a coherent cell sheet following wounding. This makes quantitative analysis of rates of closure much easier in the MDCK system, since the wound margin can be traced and the remaining open area easily determined from digital images at any time point.

By using this MDCK wound closure assay, we identified a new inhibitor of cell sheet migration during wound closure in MDCK cell monolayers (Table 1, Figure 1, and Figure 2). This compound (UIC-1005) is an optically active 3,4-disubstituted oxazolidinone with an α,β unsaturated *N*-acyl group (Scheme 1). Based on dose-response data, the calculated IC_{50} for inhibition of wound closure at 12 h by UIC-1005 is 14.0 μM ($\log IC_{50} \pm$ standard error of $\log IC_{50} = -4.853 \pm 0.09815$). This inhibitory effect is reversible at the biological level, since upon washing out the compound and changing to compound-free medium, the rate of wound closure recovers to the control rate. UIC-1005 does not act simply by inhibiting a serum component in the cell culture medium, since the compound also inhibits wound closure to a similar degree relative to the control in serum-free conditions.

Table 1. *UIC-1005, but not UIC-1017, inhibits wound closure in a statistically significant manner following wounding of MDCK cell monolayers.*[a]

	Probability (p) values	
Time [h]	UIC-1005 versus control	UIC-1017 versus control
2	0.01873265*	0.03461307*
4	0.00682226*	0.05726700
6	0.00053329*	0.08385675
8	0.00016039*	0.19205910
10	0.00001153*	0.21617469
12	0.00001023*	0.35035996
14	0.00000146*	0.35499359
16	0.00000064*	0.28478265
18	0.00000033*	0.30501469
30	0.00000002*	0.23193206
36	0.00000015*	0.19600091

[a] Student's t-test probability (p) values are shown for percentage wound closure data presented in Figure 2B; these results demonstrate significant differences from the control (0.1% DMSO, $n = 25$ wounded cell monolayers) for treatment with UIC-1005 (50 μM, $n = 19$) but not with UIC-1017 (50 μM, $n = 10$). UIC-1017 had no significant effect even at the highest concentration tested (500 μM). All significant differences ($p < 0.05$) from the control are indicated with an asterisk.

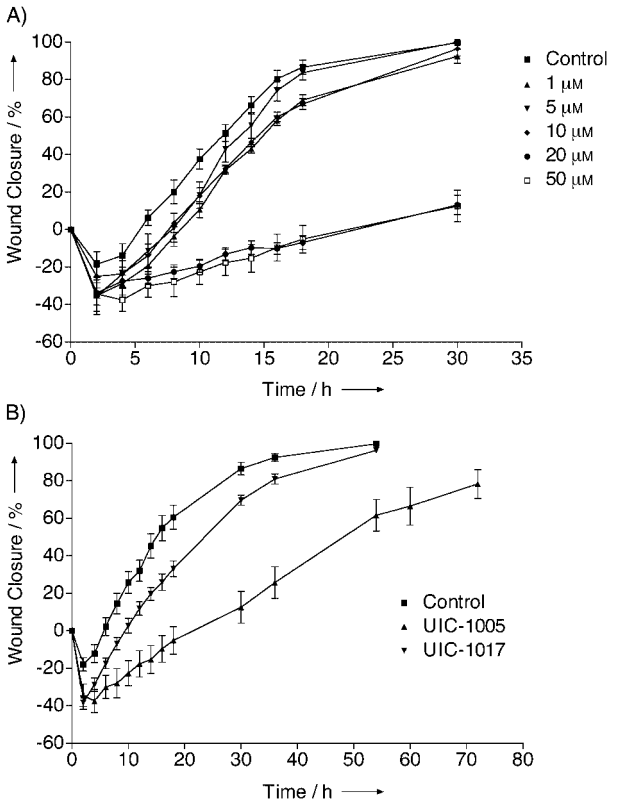

Figure 2. *Wound closure in MDCK cell monolayers in the presence or absence of UIC-1005 or UIC-1017. Values are the mean with standard error of the mean (SEM) for percentage wound closure at the times indicated. A) Time-course of wound closure for different concentrations of UIC-1005: 0.1% DMSO (n = 25 wounded cell monolayers), 1 μM (n = 9), 5 μM (n = 9), 10 μM (n = 15), 20 μM (n = 8), and 50 μM (n = 19). The calculated IC_{50} value for inhibition of wound closure at 12 h by UIC-1005 from the dose-response experiments is 14.0 μM ($\log IC_{50} = -4.853 \pm 0.09815$). Inhibition of wound closure by UIC-1005 is reversed at the biological level when the compound is washed out. B) Time-course of wound closure for the following treatments: 0.1% DMSO (control, n = 25 wounded cell monolayers), 50 μM UIC-1005 (n = 19), or 50 μM UIC-1017 (n = 10). UIC-1017 had no statistically significant effect on wound closure (see Table 1), even at the highest concentration tested (500 μM).*

Lamellipodial protrusion is thought to drive most forms of animal cell motility. At any given time in the migrating cell sheet, some cells are extending lamellipodia at the margin while others are not. Although treatment with UIC-1005 does not completely abolish formation of lamellipodia, as shown in Figure 3, it does result in significantly fewer cells extending lamellipodia at the margin (Table 2), as determined by counting the number of lamellipodial protrusions at the margin and dividing by the margin perimeter length. Therefore, inhibition of cell sheet migration by UIC-1005 may at least in part be a result of reduced formation of lamellipodia at the margin.

The course of wound closure in this assay frequently appears biphasic. In the first few hours, there is often further gapping open of the wound as cells that are damaged but still attached at the margin die and perimarginal contractile actin/myosin bundles form and help establish a stable wound margin under tension. This is followed by increasing protrusive activity at the margin and rapid closure of the wound, a process inhibited by UIC-1005. This inhibitory effect is reversible at the biological level upon washing the compound out of the medium, which indicates that inhibition is not secondary to an irreversible cellular process such as apoptosis.

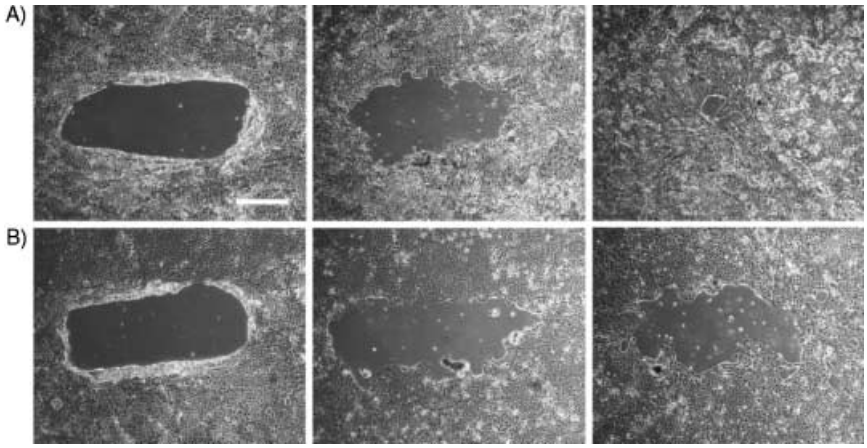

Figure 1. *UIC-1005 inhibits cell sheet migration during wound closure in MDCK cell monolayers. Representative phase-contrast micrographs of cells under the following treatment conditions: A) 0.1% dimethylsulfoxide (DMSO) control (carrier solvent control with the same final solvent concentration as in the experimental treatments) at (from left to right) 0 h, 12 h, and 36 h after wounding; B) 50 μM UIC-1005 at 0 h, 12 h, and 36 h after wounding. Scale bar = 500 μm.*

There is no evidence of toxicity or metabolic distress at concentrations at which UIC-1005 inhibits cell migration as determined by the Trypan Blue exclusion cell viability assay. Cells also remain normal in morphology with both cell–substratum and cell–cell adhesion intact after treatment with UIC-1005. Furthermore, treatment with UIC-1005 does not affect forma-

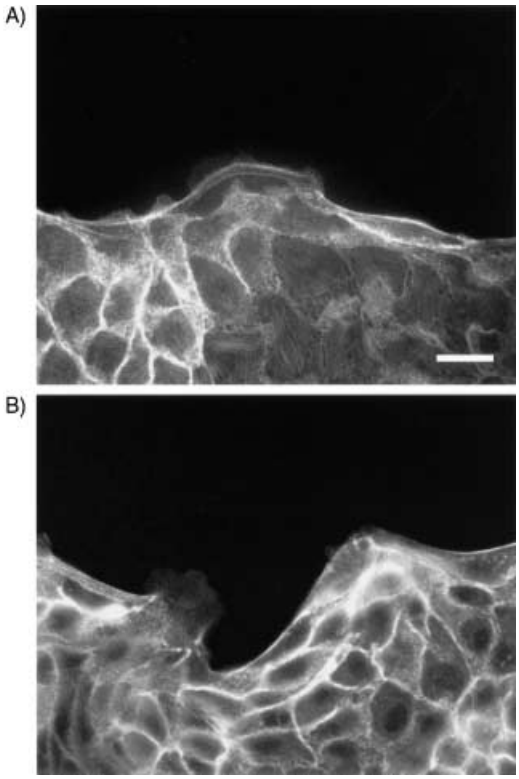

Figure 3. *UIC-1005 does not affect the formation of new filamentous actin bundles at the wound margin. Representative fluorescence micrographs of rhodamine-phalloidin-stained MDCK cell monolayers 12 h after wounding under the following treatment conditions: A) 0.1% DMSO control; B) 50 μM UIC-1005. The perimarginal actin bundles are the intensely stained structures at the wound margin parallel to the edge of the wound. Scale bar = 25 μm.*

Table 2. *UIC-1005 treatment leads to decreased formation of lamellipodial protrusions at the wound margin.*[a]

	Lamellipodial density [lamellipodia mm^{-1}]		
Time [h]	Control	UIC-1005	UIC-1017
2	0.912 ± 0.205	0.341 ± 0.119	0.563 ± 0.148
4	1.425 ± 0.199	0.573 ± 0.194*	1.139 ± 0.270
6	1.592 ± 0.313	0.563 ± 0.142*	1.289 ± 0.276
8	1.697 ± 0.244	0.938 ± 0.184*	1.196 ± 0.312
10	1.389 ± 0.226	0.803 ± 0.203	1.609 ± 0.357
12	1.272 ± 0.215	0.520 ± 0.124*	1.368 ± 0.309

[a] Lamellipodial density at the margin of MDCK cell wounds under the following treatment conditions: 0.1% DMSO (control, $n = 25$ wounded cell monolayers), 50 μM UIC-1005 ($n = 19$) or 50 μM UIC-1017 ($n = 10$). Lamellipodial density is the number of lamellipodia detected at the wound margin until closure for the times indicated divided by margin perimeter length. Values are given as the mean ± SEM. Statistically significant differences ($p < 0.05$) from the control value are indicated with asterisks.

tion of new filamentous actin bundles at the wound margin (Figure 3), a fact demonstrating that cells are still metabolically capable of forming new actin filaments, a process which requires adenosine triphosphate. These perimarginal actin bundles form rapidly after wounding of both control and UIC-1005-treated MDCK cell monolayers. Although formation of the perimarginal actin bundles is not required for wound closure in this system, these actin bundles may help to distribute force in the first row of cells from actively protruding and moving cells to less actively motile cells, thus making the closure process more regular and uniform than it would be otherwise.[28]

UIC-1005 also inhibits cell growth in MDCK cells (Figure 4A) in a biologically reversible manner (Figure 4B) at concentrations at which there is no evidence of general toxicity. As many signaling proteins are involved in both cell motility and cell cycle

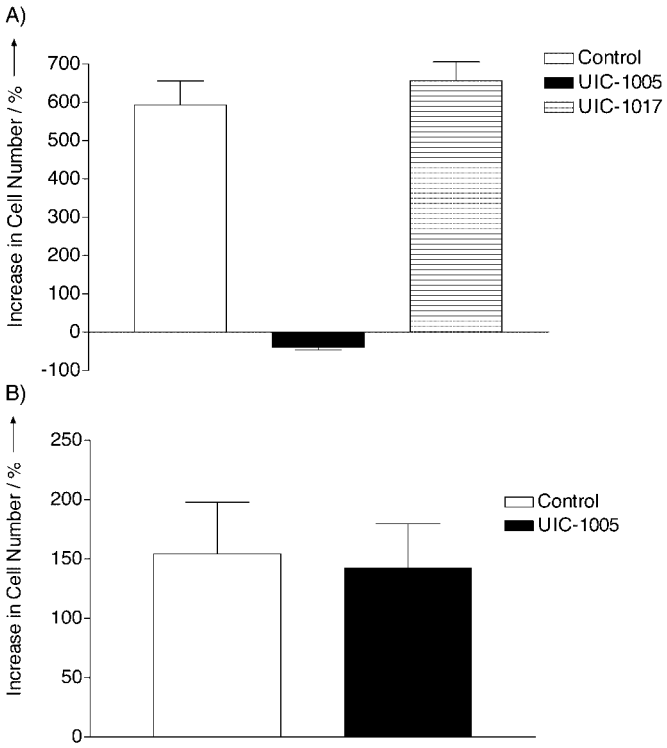

Figure 4. *A) UIC-1005 inhibits MDCK cell proliferation but UIC-1017 does not. Treatments of cells plated at a low cell density are 0.1% DMSO (control, n = 9 cultures), 50 μM UIC-1005 (n = 8), or 50 μM UIC-1017 (n = 7). Values are means with SEM of the percentage increase in cell number from 0 h to 48 h after addition of compound. B) The inhibitory effect of UIC-1005 on cell proliferation is reversible at the biological level upon washing out the compound. Values are means with SEM of the percentage increase in cell number another 48 h after replacement of medium containing 50 μM UIC-1005 (n = 8 cultures) or 0.1% DMSO (n = 9) with fresh compound-free medium.*

progression, it is probable that many of the bioactive compounds identified in a cell motility screen will also affect cell proliferation, as is the case for UIC-1005. In fact, it is known that the small GTPases Rac, Rho, and Cdc42, which are best appreciated as modulators of the actin cytoskeleton and therefore cell shape change and motility, are also involved in cell cycle progression and growth.[34] Many other known signaling proteins are involved conservatively in multiple processes, so even a highly specific inhibitor of a given signaling protein may be pleiotropic in its biological effects. Alternatively, the two inhibitory effects may be mediated by different targets. However, in the context of wound closure in MDCK cell monolayers, inhibition by UIC-1005 cannot be the result of an effect on cell proliferation, since wound closure in this system is not driven by cell proliferation but rather by cell spreading and motility.[27–29]

We have also found that UIC-1005 inhibits early development in frog embryos[35] and tissue dynamics in embryonic explants[36]

with equivalent potency. UIC-1005's effects on the frog embryo are most pronounced at stages after most embryonic cell proliferation has occurred when morphogenesis is driven principally by cell motility and cell rearrangement.

Some 3,5-disubstituted oxazolidinones,[37, 38] such as DuP-105, DuP-721,[39] eperizolid, and linezolid,[40–44] inhibit prokaryotic ribosomal protein synthesis and growth of Gram-positive bacteria such as *Staphylococcus aureus*. Another activity associated with certain oxazolidinones, such as befloxatone[45] and linezolid,[44] is inhibition of monoamine oxidase, while other oxazolidinone-containing phospholipid analogues have been shown to inhibit phospholipase A2.[46–48]

In contrast to these oxazolidinones, UIC-1005 is a non-phospholipid mimetic, 3,4-disubstituted oxazolidinone with an α,β-unsaturated *N*-acyl group. UIC-1005 does not affect the growth of either Gram-positive or Gram-negative bacteria (Table 3). Furthermore, although chiral 4-substituted oxazolidinones and α,β-unsaturated *N*-acyloxazolidinones have become widely used in asymmetric organic synthesis since their introduction by Evans and co-workers,[49–51] the present study is the first report of biological activity for these molecules. UIC-1005 therefore represents a novel class of bioactive oxazolidinone derivative.

Table 3. *UIC-1005 does not inhibit the growth of either Gram-positive or Gram-negative bacteria.*[a]

	A_{600} [absorbance units]			
	Staphylococcus aureus		*Escherichia coli*	
Time [h]	Control	UIC-1005	Control	UIC-1005
0	0.091 ± 0.002	0.117 ± 0.037	0.128 ± 0.004	0.119 ± 0.001
1	0.109 ± 0.012	0.160 ± 0.056	0.190 ± 0.004	0.215 ± 0.005
2	0.259 ± 0.024	0.332 ± 0.130	0.572 ± 0.009	0.628 ± 0.024
3	0.753 ± 0.038	0.615 ± 0.162	1.137 ± 0.018	1.127 ± 0.019
4	1.394 ± 0.060	0.937 ± 0.181	1.614 ± 0.017	1.613 ± 0.035
17			2.725 ± 0.008	2.595 ± 0.024
27	3.695 ± 0.410	3.265 ± 0.196		
31	4.067 ± 0.467	3.608 ± 0.271		
38			2.854 ± 0.023	2.795 ± 0.050

[a] Growth of *Staphylococcus aureus* (a Gram-postive bacterial species) and *Escherichia coli* (a Gram-negative bacterial species) in the presence of 0.1% DMSO (carrier solvent control) or UIC-1005 (50 μM), measured as absorbance at 600 nm (A_{600}). Values are given as the mean ± SEM for triplicate samples.

The α,β-unsaturated acyl moiety attached to the nitrogen atom of the oxazolidinone ring of UIC-1005 potentially functions as a reactive electrophile, a possible Michael acceptor. UIC-1005 therefore has the potential to form a covalent complex with a nucleophilic cellular target by 1,4-addition of the nucleophile to the α,β-unsaturated acyl group (Scheme 1). The observation that the closest saturated analogue, UIC-1017 (Scheme 1), displays no statistically significant bioactivity in either wound closure (Table 1, Figure 2B) or cell proliferation (Figure 4A) assays, even at the highest concentration tested (500 μM), is consistent with this hypothesis.

Table 1 shows that treatment with UIC-1017 does not result in statistically significant differences in percentage wound closure from the control over the course of the experiment. The rate of wound closure, which corresponds to the slope of the curves in Figure 3B, is also the same as the control rate. The only time when treatment with UIC-1017 displays a statistically significant difference in percentage closure from the control is at 2 h after wounding. We have found that percentage closure values at 2 h are always more variable and perhaps less meaningful than later, regardless of treatment, as a result of small differences in the original size of the scrape wounds generated and the degree to which a given wound gap initially opens. All other percentage closure values for treatment with UIC-1017 are within the range of experimental error for and statistically indistinguishable from the control according to the Student's *t*-test.

UIC-1017 is the product of hydrogenation of UIC-1005, that is, identical in structure except that it lacks the C2′—C3′ double bond, which makes it chemically unreactive towards nucleophiles. A preliminary structure – activity relationship study with other analogues in which the electrophilicity of the C3′ carbon is altered also indicates a correlation between the potential for nucleophilic attack at the C3′ atom and biological activity. A complete study is currently underway.

Although a biochemical interaction based on addition of a nucleophilic target to the compound would be covalent and likely stable, the inhibitory effects of UIC-1005 on both wound closure and cell proliferation assays are biologically reversible. Our assays are conducted in whole cells in which new biosynthesis can occur, whereas our hypothesis about the interaction concerns a potential biochemical interaction. While not ruling out alternative hypotheses, this may be as a result of the biological turnover of the cellular target. If it is continuously synthesized in the cell, washing out compound allows newly synthesized target to fulfill its cellular function without being inhibited. Alternatively, the interaction could be labile and chemically reversible.

The cellular target may be a protein or other biological macromolecule containing a functionally important nucleophile. It is also possible that the immediate target is instead an endogenous nucleophilic small molecule, such as glutathione or an intracellular metabolite; this would result in a conjugate that would then mediate the biological effects of treatment, presumably by interaction with a protein. Another possibility, of course, is that the α,β-unsaturated *N*-acyl group of UIC-1005 may be important for a reason unrelated to its potential reactivity, such as the reduced conformational flexibility that it would confer.

Purification of the cellular target(s), characterization of its interaction with UIC-1005, and analysis of its rate of biosynthesis and turnover will serve to definitively answer these questions. Moreover, identification of UIC-1005's specific cellular target may provide new information on the signal transduction pathways leading to epithelial cell sheet migration. Efforts to identify the target of this small molecule are now in progress.

Conclusion

We have reported a system for rapid screening of chemical libraries for compounds that affect epithelial cell sheet migration during wound closure. By using this assay, we have discovered a

new cell-permeant inhibitor of cell sheet migration. This small molecule (UIC-1005) is a 3,4-disubstituted oxazolidinone with an electrophilic α,β-unsaturated *N*-acyl group that is required for activity. The compound also inhibits cell growth in an epithelial cell proliferation assay. It exhibits no general toxicity at concentrations at which it inhibits cell sheet migration and growth. Unlike some 3,5-disubstituted oxazolidinones, the compound displays no antibacterial activity. UIC-1005 represents a new class of bioactive oxazolidinone derivative that may prove to be useful in understanding and controlling the signaling pathways leading to cell migration. This and related molecules may also be of value as potential leads for the development of therapeutic agents such as inhibitors of angiogenesis and cancer metastasis.

Experimental Section

Chemical synthesis:

(4*S*)-3-[(*E*)-But-2-enoyl]-4-benzyl-2-oxazolidinone (UIC-1005): UIC-1005 was synthesized by the procedure of Evans et al.[51] *n*-Butyllithium (1.6 M in hexanes, 3.5 mL, 5.6 mmol) was added dropwise to a solution of (4*S*)-4-benzyl-2-oxazolidinone (1.0 g, 5.6 mmol) in anhydrous tetrahydrofuran (20 mL) and cooled to $-78\,^{\circ}$C. After 30 min, (*E*)-crotonyl chloride (59 μL, 6.2 mmol) was added. The reaction mixture was stirred for an additional 30 min at $-78\,^{\circ}$C and then allowed to warm to room temperature slowly. The reaction was quenched with aqueous NH_4Cl (4 mL), diluted with diethyl ether, and washed with saturated $NaHCO_3$, H_2O, and brine. The organic layer was dried (Na_2SO_4) and evaporated under reduced pressure. Flash chromatography over silica gel with ethyl acetate/hexane (1:3) as eluent provided UIC-1005 (1.2 g, 87% yield) as a white solid. M.p. 83 °C; $[\alpha]_D^{25} = +77.7$ ($c = 2.00$ in $CHCl_3$); ^{1}H NMR (400 MHz, $CDCl_3$): $\delta =$ 7.36 – 7.15 (m, 7H; Ph, CH=CH), 4.75 – 4.70 (m, 1H; CHN), 4.23 – 4.15 (m, 2H; CH_2O), 3.33 (dd, 1H, $J = 3.3$, 13.4 Hz; C*H*HPh), 2.79 (dd, 1H, $J = 9.5$, 13.4 Hz; CH*H*Ph), 1.98 (dd, 3H, $J = 1.0$, 6.2 Hz; CH_3) ppm; ^{13}C NMR (100 MHz, $CDCl_3$): $\delta =$ 164.69, 153.51, 146.95, 135.28, 129.37, 128.86, 127.23, 121.74, 66.01, 55.20, 37.79, 18.50 ppm; IR (KBr): $\tilde{\nu} =$ 3027, 2922, 2539, 1772, 1682, 1351, 1209 cm^{-1}; HRMS (EI): *m/z* calcd for $C_{14}H_{16}O_3N$ $[M+H]^+$: 246.1125; found: 246.1127.

(4*S*)-3-Butyryl-4-benzyl-2-oxazolidinone (UIC-1017): 10% (w/w) Pd/C (100 mg) was added to a solution of UIC-1005 (1.0 g, 4.08 mmol) in ethyl acetate (20 mL). The reaction mixture was stirred in a hydrogen atmosphere (1 atm) for 1 h, filtered through Celite, and the filtrate was concentrated. Flash chromatography over silica gel with hexane/ethyl acetate (4:1) as eluent provided UIC-1017 (980 mg, 97% yield) as a colorless syrup. $[\alpha]_D^{25} = +71.0$ ($c = 0.20$ in $CHCl_3$); ^{1}H NMR (400 MHz, $CDCl_3$): $\delta = 7.44 - 7.19$ (m, 5H; Ph), 4.70 – 4.64 (m, 1H; CHN), 4.22 – 4.14 (m, 2H; CH_2O), 3.29 (dd, 1H, $J = 3.2$, 13.2 Hz; C*H*HPh), 3.01 – 2.83 (m, 2H; CH_2CO), 2.77 (dd, 1H, $J = 9.6$, 13.2 Hz; CH*H*Ph), 1.77 – 1.68 (m, 2H; CH_2CH_3), 1.03 (t, 3H, $J = 7.4$ Hz; CH_3) ppm; ^{13}C NMR (100 MHz, $CDCl_3$): $\delta =$ 173.12, 153.38, 135.24, 129.42, 128.85, 127.23, 66.06, 55.04, 37.84, 37.29, 17.61, 13.60 ppm; IR (film): $\tilde{\nu} =$ 2963, 1779, 1699, 1387, 1215, 771 cm^{-1}; HRMS (EI): *m/z* calcd for $C_{14}H_{17}O_3N$ $[M]^+$: 247.1203; found: 247.1202.

Cell culture conditions: MDCK cells (American Type Culture Collection cell line CCL-34) were cultured in minimum essential medium (with Earle's balanced salts, nonessential amino acids, L-glutamine, and sodium pyruvate) supplemented with 10% (v/v) newborn calf serum at 37 °C and 5% CO_2. Main cultures were grown in either 25- or 75-cm^3 tissue culture flasks with medium changes every 2 days. When cultures were ≈75% confluent, cells were passaged by rinsing twice with 1 × phosphate-buffered saline (PBS) and treating with a solution of 0.05% (w/v) trypsin/0.02% (w/v) ethylenediaminetetraacetic acid (EDTA) in PBS to detach cells from the flasks. After cells were detached, an equal volume of serum-containing medium was added to inhibit the trypsin, and cell density was determined with a hemacytometer. Cells were replated following dilution in fresh medium in new tissue culture flasks for continued culture and multiwell tissue culture plate experiments. No culture used exceeded 15 passages. Experimental cultures were grown in 12-, 24-, 48-, or 96-well tissue culture plates with medium changes every 2 days.

Wound closure assay and compound screening: MDCK cells were plated in multiwell tissue culture plates and cultured at 37 °C and 5% CO_2 with medium changes every 2 days until confluent. When the cultures reached confluence, the medium was changed again, and all experimental treatments were started a day later. Compounds were solubilized in dimethylsulfoxide (DMSO) and added with fresh medium to cell cultures at an initial screening concentration of 100 μM. Controls consisted of parallel wells to which DMSO carrier solvent alone was added at the same concentration as that added with experimental treatments (not exceeding 0.1% (v/v)). DMSO alone had no detectable effect on the cells at this concentration. Cell monolayers were scraped 30 min later with a micropipette and ultramicro tips to produce small wounds of consistent shape and size (oval-shaped wounds with an initial open area of ≈0.5 mm^2 to ≈1 mm^2).

Progress of wound closure in initial high-throughput screening assays was examined at set time intervals following wounding by observation with a microscope. Wounds were recorded as either open or closed at the times of observation, thereby allowing possible inhibitory or acceleratory effects on wound closure relative to parallel controls to be detected. We found that one person could carry out at least 960 unique treatments (wells) per day with this assay. Compounds can be screened individually or in groups of 10 or 100 per well for even higher throughput. When screening pooled compounds, pools that have activity can be subsequently subdivided into their individual molecules for a second screen to identify the unique active compound(s).

Compounds that exhibited biological activity in the initial assay were tested further at a range of concentrations with a greater sample size to generate dose-response data with statistical relevance. Digital images of the wounded MDCK cell monolayers were taken every 2 h for 18 h and then at 30 h, 36 h, 54 h, 60 h, and 72 h following wounding. In addition, the number of lamellipodia at the wound margin was counted at these times. Reversibility of compound effects in this assay was examined by treating with compound and scraping the cell monolayer as before, then at later times washing the monolayer twice with PBS, adding fresh compound-free medium, and determining the rate of closure after that point. The rate of closure corresponds to the slope of the curve in graphs of percentage closure over time.

Imaging and analysis: Wound closure assays were performed by using either a Zeiss Axiovert 200 inverted microscope with a Zeiss AxioCam CCD camera and Improvision OpenLab imaging software running on an Apple Power Mac G4 computer or a Zeiss Axiovert 25 inverted microscope with a Roper Scientific/Photometrics CoolSNAP-Pro CCD camera and Roper Scientific/Photometrics RS Image software on an Apple Power Mac G4 computer. Subsequent morphometric analyses with the digital images were performed by using the public domain NIH Image program (developed at the US National Institutes of Health and available on the Internet at http://rsb.info.nih.gov/nih-image/). These analyses entailed tracing the

wound margin in each of the digital images to determine the length of the margin perimeter and the remaining open area. Microsoft Excel and GraphPad Prism software were used for routine tabulation, analysis, and graphing of the data. The dose-response data was used to determine the IC_{50} for inhibition of wound closure by UIC-1005 with GraphPad Prism software.

Filamentous actin staining: MDCK cell monolayers on glass coverslips were fixed with 3.7% (w/v) formaldehyde in PBS 12 h after wounding. Cells were permeabilized with 0.1% (w/v) Triton X-100 in PBS, stained with 50 nM tetramethylrhodamine-conjugated phalloidin in PBS, and then washed twice with PBS. Coverslips were mounted in 90% (v/v) glycerol/10% (v/v) 10 × PBS with 2 mg mL^{-1} *p*-phenylenediamine on glass slides and then examined by fluorescence microscopy.

MDCK cell proliferation: MDCK cells were plated in 12-well tissue culture plates at a low density (1×10^4 cells per well). Cells were allowed to attach and begin to grow for 48 h before the start of the experiment. Fresh medium with or without compound was then added, and cells were incubated for 48 h. At both 0 h and 48 h, some of the parallel wells for control and compound treatments were washed twice with PBS and treated with trypsin/EDTA solution to detach the cells. An equal volume of medium was added. Cells were collected and counted with a hemacytometer. For testing reversibility, some of the parallel cultures for both control and compound treatments were grown for another 48 h after washing twice with PBS and replacing medium with fresh compound-free medium. At both the time of washing out and 48 h later, some of the parallel wells for control and compound treatments were washed twice with PBS, detached from the plates with trypsin/EDTA solution, and the number of cells was counted.

Bacterial growth: *Staphylococcus aureus* or *Escherichia coli* (DH5α strain) were grown in Luria–Bertani (LB) medium for 12 h at 37 °C in a shaking incubator. Dilutions into fresh LB medium with 0.1% DMSO (carrier solvent control) or 50 μM UIC-1005 were made to an absorbance at 600 nm of ≈0.1. Bacteria were incubated at 37 °C with shaking during the experiment, and A_{600} measurements were made at set time intervals during the log growth phase until the plateau phase was reached.

We wish to acknowledge Dr. Khaja Azahr Hussein for preliminary syntheses and Prof. Tapan Misra and Prof. Richard Kassner for providing Staphylococcus aureus *and* Escherichia coli, *respectively. This work was supported by the University of Illinois at Chicago (UIC), the UIC Campus Research Board, and the National Cancer Institute of the National Institutes of Health (Grant no.: CA095177 to G.F.).*

[1] J. R. Bartles, *Curr. Opin. Cell Biol.* **2000**, *12*, 72.
[2] G. G. Borisy, T. M. Svitkina, *Curr. Opin. Cell Biol.* **2000**, *12*, 104.
[3] H. Chen, B. W. Bernstein, J. R. Bamburg, *Trends Biochem. Sci.* **2000**, *25*, 19.
[4] R. D. Mullins, *Curr. Opin. Cell Biol.* **2000**, *12*, 91.
[5] T. D. Pollard, *Trends Biochem. Sci.* **2000**, *25*, 607.
[6] M. A. Wear, D. A. Schafer, J. A. Cooper, *Curr. Biol.* **2000**, *10*, R891.
[7] J. Condeelis, *Trends Cell Biol.* **2001**, *11*, 288.
[8] D. Pantaloni, C. Le Clainche, M. F. Carlier, *Science* **2001**, *292*, 1502.
[9] T. P. Stossel, J. Condeelis, L. Cooley, J. H. Hartwig, A. Noegel, M. Schleicher, S. S. Shapiro, *Nat. Rev. Mol. Cell Biol.* **2001**, *2*, 138.
[10] J. V. Small, T. Stradel, E. Vignal, K. Rottner, *Trends Cell Biol.* **2002**, *12*, 112.
[11] A. Hall, C. D. Nobes, *Philos. Trans. R. Soc. Lond. B. Biol. Sci.* **2000**, *355*, 965.
[12] A. A. Schmitz, E. E. Govek, B. Bottner, L. Van Aelst, *Exp. Cell Res.* **2000**, *261*, 1.
[13] A. J. Ridley, *J. Cell Sci.* **2001**, *114*, 2713.
[14] A. J. Ridley, *Trends Cell Biol.* **2001**, *11*, 471.
[15] M. L. Coleman, C. J. Marshall, *Nat. Cell Biol.* **2001**, *3*, E250.
[16] E. H. Danen, K. M. Yamada, *J. Cell Physiol.* **2001**, *189*, 1.
[17] A. J. Ridley, *Dev. Cell* **2001**, *1*, 160.
[18] M. Fukata, K. Kaibuchi, *Nat. Rev. Mol. Cell Biol.* **2001**, *2*, 887.
[19] P. Janmey, *Ann. Rev. Physiol.* **1994**, *56*, 169.
[20] G. Fenteany, S. Zhu, *Curr. Topics Med. Chem.*, in press.
[21] J. A. Cooper, *J. Cell Biol.* **1987**, *105*, 1473.
[22] I. Spector, *Science* **1983**, *219*, 493.
[23] M. R. Bubb, A. M. Senderowicz, E. A. Sausville, K. L. Duncan, E. D. Korn, *J. Biol. Chem.* **1994**, *269*, 14869.
[24] M. Uehata, T. Ishizaki, H. Satoh, T. Ono, T. Kawahara, T. Morishita, H. Tamakawa, K. Yamagami, J. Inui, M. Maekawa, S. Narumiya, *Nature* **1997**, *389*, 990.
[25] M. Saitoh, M. Naka, H. Hidaka, *Biochem. Biophys. Res. Commun.* **1986**, *140*, 280.
[26] J. R. Peterson, R. S. Lokey, T. J. Mitchison, M. W. Kirschner, *Proc. Natl. Acad. Sci. USA* **2001**, *98*, 10624.
[27] H. T. Sponsel, R. Breckon, W. Hammond, R. J. Anderson, *Am. J. Physiol.* **1994**, *267*, F257.
[28] G. Fenteany, P. A. Janmey, T. P. Stossel, *Curr. Biol.* **2000**, *10*, 831.
[29] R. Farooqui, S. Zhu, G. Fenteany, unpublished results.
[30] A. Jacinto, A. Martinex-Arias, P. Martin, *Nat. Cell Biol.* **2001**, *3*, E117.
[31] S. Kartha, F. G. Toback, *J. Clin. Invest.* **1992**, *90*, 288.
[32] K. Nakae, Y. Yoshimoto, T. Sawa, Y. Homma, M. Hamada, T. Takeuchi, M. Imoto, *J. Antibiot. (Tokyo)* **2000**, *53*, 1130.
[33] Y. Takemoto, K. Nakae, M. Kawatani, Y. Takahashi, H. Naganawa, M. Imoto, *J. Antibiot. (Tokyo)* **2001**, *54*, 1104.
[34] M. F. Olson, A. Ashworth, A. Hall, *Science* **1995**, *269*, 1270.
[35] S. Anjum, S. V. Ankala, G. Fenteany, unpublished results.
[36] Z. M. Altan, G. Fenteany, unpublished results.
[37] D. J. Diekema, R. N. Jones, *Lancet* **2001**, *358*, 1975.
[38] G. A. Evans, *Curr. Infect. Dis. Rep.* **2002**, *4*, 17.
[39] A. M. Slee, M. A. Wuonola, R. J. McRipley, I. Zajac, M. J. Zawada, P. T. Bartholomew, W. A. Gregory, M. Forbes, *Antimicrob. Agents Chemother.* **1987**, *31*, 1791.
[40] S. J. Brickner, D. K. Hutchinson, M. R. Barbachyn, P. R. Manninen, D. A. Ulanowicz, S. A. Garmon, K. C. Grega, S. K. Hendges, D. S. Toops, C. W. Ford, G. E. Zurenko, *J. Med. Chem.* **1996**, *39*, 673.
[41] R. N. Jones, D. M. Johnson, M. E. Erwin, *Antimicrob. Agents Chemother.* **1996**, *40*, 720.
[42] G. French, *Int. J. Clin. Pract.* **2001**, *55*, 59.
[43] H. B. Fung, H. L. Kirschenbaum, B. O. Ojofeitimi, *Clin. Ther.* **2001**, *23*, 356.
[44] R. Norrby, *Expert Opin. Pharmacother.* **2001**, *2*, 293.
[45] V. Rovei, D. Caille, O. Curet, D. Ego, F. X. Jarreau, *J. Neural Transm. Suppl.* **1994**, *41*, 339.
[46] T. Tani, S. Fujii, S. Inoue, K. Ikeda, S. Iwama, T. Matsuda, S. Katsumura, Y. Samejima, K. Hayashi, *J. Biochem. (Tokyo)* **1995**, *117*, 176.
[47] S. Iwama, T. Matsuda, S. Katsumura, T. Tani, S. Fujii, K. Ikeda, H. Takehara, *Bioorg. Med. Chem.* **1995**, *3*, 1397.
[48] S. Iwama, M. Segawa, S. Fujii, K. Ikeda, S. Katsumura, *Bioorg. Med. Chem. Lett.* **1998**, *8*, 3495.
[49] D. A. Evans, T. R. Taber, *Tetrahedron Lett.* **1980**, *21*, 4675.
[50] D. A. Evans, J. Bartroliu, T. L. Shih, *J. Am. Chem. Soc.* **1981**, *103*, 2127.
[51] D. A. Evans, K. T. Chapman, J. Bisaha, *J. Am. Chem. Soc.* **1988**, *110*, 1238.

Received: May 10, 2002 [F413]